

ONSET OF CONVECTION IN A HORIZONTAL WATER LAYER WITH MAXIMUM DENSITY EFFECTS

G. P. MERKER,* P. WAAS and U. GRIGULL

Lehrstuhl A für Thermodynamik, Technische Universität München,
 8000 Munich 2, P.O.B. 202420, W. Germany

(Received 20 July 1978 and in revised form 22 August 1978)

Abstract—The onset of convection in a horizontal water layer with regard to the density anomaly (near 4°C) is studied using linear stability analysis. The resulting perturbation equations are solved with the aid of Galerkin's method. With the choice of reasonable test functions, it is shown that seven terms are sufficient for an approach close to 1%. The results are represented in stability diagrams, $Ra = Ra(T_1, T_2)$ where T_1 and T_2 are the temperatures of the lower and upper wall, respectively. The nonlinear density–temperature relation is approximated by three different polynomials having 2, 3 and 5 terms. Assuming the fifth order polynomial to be exact, the critical Rayleigh numbers calculated with the simple parabolic relation are about 10% too large. This discrepancy is reduced to approximately +3% by adding a cubic term to the density–temperature relation.

NOMENCLATURE

<p>a, thermal diffusivity;</p> <p>A, matrix element;</p> <p>B_i, coefficients of density–temperature relation;</p> <p>C_i, D_m, coefficients;</p> <p>f, nondimensional density–temperature relation;</p> <p>$F(z), G(z)$, perturbation functions;</p> <p>g, gravity;</p> <p>Ga, Galileo number = gH^3/av;</p> <p>H, height of water layer;</p> <p>$H(x, y)$, perturbation function;</p> <p>I, K, integral expression;</p> <p>k, wave number;</p> <p>N_i, nonlinearity;</p> <p>n, number of Galerkin terms;</p> <p>p, power of density–temperature relation;</p> <p>P, pressure;</p> <p>Pr, Prandtl number = v/a;</p> <p>\dot{q}, heat flux density;</p> <p>Q, internal heat source rate;</p> <p>Ra, Rayleigh number (gH^3/av)β;</p> <p>t, time;</p> <p>T, temperature;</p> <p>\mathbf{u}, = (u, v, w) velocity;</p> <p>\mathbf{x}, = (x, y, z) Cartesian coordinates.</p>	<p>κ, nondimensional internal heat source rate;</p> <p>λ, thermal conductivity;</p> <p>ν, kinematic viscosity;</p> <p>ρ, density;</p> <p>σ, stability parameter;</p> <p>τ, time, nondimensionalized by H^2/a;</p> <p>ϕ, ψ, test functions;</p> <p>∇, Nabla operator;</p> <p>∇^2, Laplace operator;</p> <p>∇_2^2, two-dimensional Laplace operator.</p> <p>Superscripts</p> <p>$\hat{}$, perturbed value;</p> <p>$\bar{}$, unperturbed value.</p>
---	--

Greek symbols

β ,	coefficient of thermal expansion;
θ ,	= $(T_1 - T)/\vartheta$ nondimensional temperature;
ϑ ,	= $\begin{cases} T_1 - T_2 & \text{isothermal walls} \\ \dot{q}H/\lambda & \text{isoflux walls,} \end{cases}$
	reference temp.;

1. INTRODUCTION

TO REDUCE the heat waste of nuclear and thermal power plants, the construction of artificial lakes as heat stores has been in discussion for several years. These heat stores are filled during the summer months with the warmed up cooling water from thermal power plants. After a storage period of some months, hot water is taken from the storage to supply the district heating system during winter months. During this period, the cool return stroke enters the storage at the bottom to be used during the filling period as cooling water in the power plants. Due to inevitable external heat losses and internal temperature differences an internal heat exchange by conduction and convection occurs during the storage period. Whereas the effect of heat conduction can be easily described the convection process still yields some unsolved problems, due to the complex governing equations, the stability problems involved and the density anomaly of water, Straub [1]. Therefore, the present work concentrates on the onset of convection in water at temperatures where the density anomaly has to be taken into

*Since 1 April, 1978, Motoren und Turbinen Union, MTU-München, 8000 Munich 50, P.O.B. 500640, West-Germany.

account. In a water layer of height H and infinite horizontal dimensions which is cooled from above or heated from below convection occurs if the vertical temperature gradient exceeds a certain, i.e. critical, value. This is usually expressed by a Rayleigh-number whose critical value is 1708 in the mentioned classical problem. Benard [2] was probably the first who observed the regular cell structure for $Ra > 1708$ (it has been pointed out by some authors that the cells he visualized, where due to surface tension effects rather than thermal convection) whereas early analytical considerations were made by Rayleigh [3] and Jeffreys [4]. This classical problem has been studied intensively ever since. The results are summarized in the famous book by Chandrasekhar [5] and recently by Koschmieder [6]. More recently the problem has also been treated by Joseph [7].

In the above problem, it is assumed that the temperature gradient is constant and the density is a linear function of temperature. For water with its density maximum near 4°C the density-temperature relation is no more linear and may be approximated by a polynomial of degree p . Hence, even for a constant temperature gradient the density profile is a nonlinear function of the vertical coordinate z . The differences to the classical problem can be seen by considering the melting of an ice-layer and the freezing of a water layer.

The temperature- and density profiles in a melting ice layer heated from below and from above are shown in Figs. 1 and 2. Figure 1 shows the conduction profiles in the water layer, $T_2 = 0^\circ\text{C}$, by heating from below, $T_1 > 0^\circ\text{C}$. It is seen that the water layer is stably stratified as long as $T_1 < 4^\circ\text{C}$ and unstably for $T_1 > 4^\circ\text{C}$. It should be noted that the water-layer between the ice-surface and the 4°C isotherm is always stable. The height of the unstable layer increases with increasing wall temperature T_1 . Figure 2 shows the conduction profiles in a water layer, $T_1 = 0^\circ\text{C}$, by heating from above, $T_2 > 0^\circ\text{C}$. In contrast to Fig. 1, the height of the unstable layer decreases with increasing wall temperature T_2 . For arbitrary temperatures T_1 and T_2 , one obtains the principle stability diagram shown in Fig. 4 where $\beta_1 = \beta(T_1)$ and $\beta_2 = \beta(T_2)$ are the isothermal expansion coefficients. The Rayleigh numbers Ra_1 and Ra_2 are defined with β_1 and β_2 respectively. It is seen that regions where $Ra_1, Ra_2 < 0$ are stably and those where $Ra_1, Ra_2 > 0$ are unstably stratified. Regions where $Ra_1 \cdot Ra_2 < 0$ are partially unstably/stably stratified.

The influence of the density anomaly on the onset of convection has been studied by several authors. Using a parabolic $\rho(T)$ -function, Veronis [8] considered two cases: temperature of the lower wall equal to 0°C and temperature of the upper wall either equal to 4 or 8°C.

With the aims of linear stability theory he obtained $13.43 \times \pi^4$ and $87.18 \times \pi^4$, respectively for the critical Rayleigh numbers. The Rayleigh number

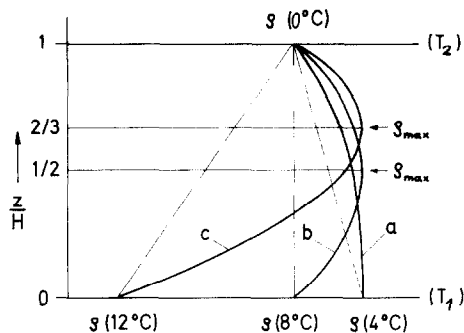


FIG. 1. Conduction density profiles in a melting ice layer heated from below, $T_2 = 0^\circ\text{C}$. (a) $T_1 = 4^\circ\text{C}$: stable water layer; (b) $T_1 = 8^\circ\text{C}$: {upper $\frac{1}{2}$ is stably/lower $\frac{1}{2}$ is unstably} stratified; (c) $T_1 = 12^\circ\text{C}$: {upper $\frac{1}{3}$ is stably/lower $\frac{2}{3}$ are unstably} stratified.

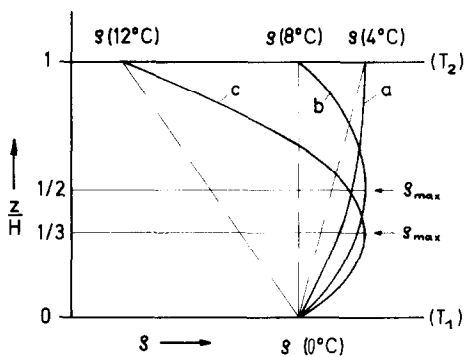


FIG. 2. Conduction density profiles in a melting ice layer heated from above, $T_1 = 0^\circ\text{C}$. (a) $T_2 = 4^\circ\text{C}$: unstable water layer; (b) $T_2 = 8^\circ\text{C}$: {upper $\frac{1}{2}$ is stably/lower $\frac{1}{2}$ is unstably} stratified; (c) $T_2 = 12^\circ\text{C}$: {upper $\frac{2}{3}$ are stably/lower $\frac{1}{3}$ is unstably} stratified.

is constructed with the height of the unstable water-layer. By adding a cubic term to the density temperature function Sun *et al.* [9] extended the work of Veronis and predicted a stability-diagram valid in the temperature region 0–35°C. Seki *et al.* [10] also used a cubic polynomial, but they defined different Rayleigh numbers for the regions $T < 4^\circ\text{C}$ and $T > 4^\circ\text{C}$. Legros *et al.* [11] considered a sixth order polynomial. Their results are in good agreement with those obtained by Veronis. Wu *et al.* [12] predicted stability curves for the onset of thermal convection including surface tension effects. At very high supercritical Rayleigh numbers Boger *et al.* [13] observed an oscillating water-ice interface in melting and freezing experiments. Furthermore, they conclude that the critical Rayleigh number - defined with the height of the unstable layer - is approximately 1700. Yen [14] and Yen *et al.* [15] observed a regular cell structure in a melting ice layer heated from below. Furthermore, they have shown that the critical Rayleigh number is not a single constant but depends on the wall temperature. Tankin *et al.* [16] and Farhadieh *et al.* [17] studied the influence of convection on the geometrical structure of the ice-surface. In freezing a water layer by cooling from below the observed critical Rayleigh number was

about 480. Numerical and experimental studies with a melting ice layer heated from above have been carried out by Seki *et al.* [18]. The observed critical Rayleigh numbers were between 200 and 10^5 where the wall temperatures varied between 1 and 15°C.

In all these papers, the critical Rayleigh number is defined with the height of the unstable layer. Compared to the classical problem this height is not known in advance but can be calculated from the density–temperature relation.

In our opinion this situation is rather unsatisfactory. It can be improved by defining a modified Rayleigh number introducing the height of the complete fluid layer rather than the height of the unstable layer, Merker *et al.* [19]. Furthermore, it can be shown that the critical Rayleigh number depends on the thermal and hydrodynamical boundary conditions (like the classical problem) and due to the density anomaly a second parameter besides the Rayleigh number is necessary to describe the onset of convection.

The present paper concentrates on the study of the onset of convection in a water layer near temperatures where the density anomaly can not be neglected. In contrast to the papers mentioned above, the Rayleigh number is defined with the height of the water layer rather than the height of unstable part only. The discrepancies in the calculated critical Rayleigh numbers due to different polynomials used for approximating the density temperature relation are discussed in some detail. Furthermore, it is shown that the approach with the first term in Galerkin's method is very limited in the present problem.

2. MATHEMATICAL FORMULATION OF THE PROBLEM

The system that we consider is shown schematically in Fig. 3. It consists of a horizontal water-layer of infinite horizontal length and finite height H which is bounded by an upper and lower wall. The walls are rigid, no-slip boundaries which are held either at different, but uniform temperatures, T_1 and T_2 , with $T_1 \geq T_2$ or at which a uniform heat flux, $\dot{q}_1 = \dot{q}_2$, is maintained.

Subject to the usual Boussinesq approximation,* the transient equations governing this system may be expressed (see [20, 21]) as

$$\nabla \mathbf{u} = 0 \tag{1}$$

$$\frac{D\mathbf{u}}{Dt} = \left(\frac{\rho}{\rho_0} - 1 \right) \mathbf{g} - \frac{1}{\rho_0} \nabla P + \nu \nabla^2 \mathbf{u} \tag{2}$$

$$\frac{DT}{Dt} = a \nabla^2 T \tag{3}$$

$$\rho = \rho(T) \tag{4}$$

with

$$\frac{D}{Dt} \equiv \frac{\partial}{\partial t} + \mathbf{u} \cdot \nabla.$$

*This is named Oberbeck–Boussinesq approximation by Joseph [7]. He gives also some interesting historical notes.

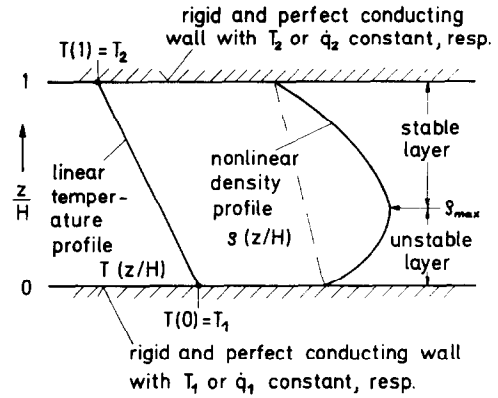


FIG. 3. Schematic diagram of the water layer.

The validity of the Boussinesq-approximation and the assumption of constant fluid properties are intensively discussed in [7, 22–24] and are therefore not repeated here.

In the present case, the density can be considered as a function of the temperature only. Hence, the equation of state reduces to a density–temperature function which can be approximated by a polynomial of order p [25, 26].

$$\frac{\rho(T)}{\rho_0} = 1 + B_1 T + B_2 T^2 + \dots = \sum_{i=0}^p B_i T^i \tag{5}$$

with T in degrees Celsius and $B_0 \equiv 1$.

With this relation, one obtains for the coefficient of thermal expansion:

$$\begin{aligned} \beta &= -\frac{1}{\rho} \left(\frac{\partial \rho}{\partial T} \right)_p \\ &= -\frac{1}{\rho} (B_1 + 2B_2 T + 3B_3 T^2 + \dots). \end{aligned} \tag{6}$$

Since the density of water decreases less than 1% as the temperature increases from 4 to 40°C, the density appearing in (6) can be considered as a constant, ρ_0

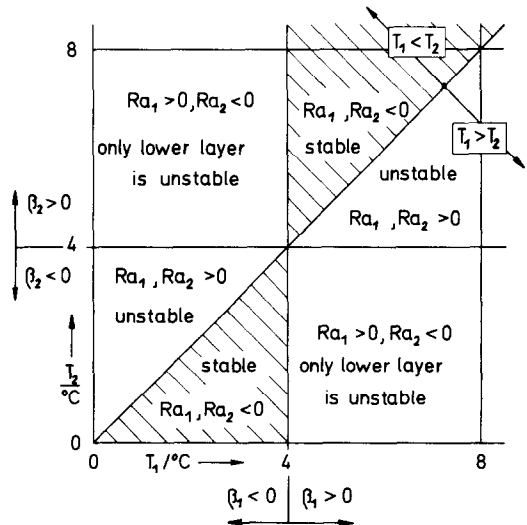


FIG. 4. Principal stability diagram.

Table 1. Coefficients for density-temperature polynomials, $\rho(T)/\rho_0 - 1$

	$n = 2$	$n = 3$ $T_i = 10^\circ\text{C}$	$n = 3$ $T_i = 20^\circ\text{C}$	$n = 5^*$
B_1	6.62105×10^{-5}	6.59706×10^{-5}	6.85650×10^{-5}	6.79939×10^{-5}
B_2	-8.27631×10^{-6}	-8.82308×10^{-6}	-8.82063×10^{-6}	-9.10749×10^{-6}
B_3		9.61265×10^{-8}	4.16668×10^{-8}	1.00543×10^{-7}
B_4				-1.12689×10^{-9}
B_5				6.59285×10^{-12}

* Values taken from Wagenbreth *et al.* [26].

$= \rho(0^\circ\text{C})$. It is evident that this simplification is in agreement with the Boussinesq-approximation.

Hence, one obtains

$$\beta = -\frac{1}{\rho_0} \sum_{i=1}^p i B_i T^{i-1}. \quad (7)$$

The value of the density maximum of water is $\rho_{\max} = 999.9720 \text{ kg/m}^3$ where the temperature lies between $3.9557 \leq T_{\max} \leq 4.0043^\circ\text{C}$. To determine the coefficients B_i we assume $T(\rho_{\max}) = 4^\circ\text{C}$. With the additional density value $\rho(0^\circ\text{C}) = 999.8396 \text{ kg/m}^3$ one obtains the coefficients B_1 and B_2 for the simple parabolic density-temperature relation. A polynomial of order three is obtained by using in addition the value $\rho(10^\circ\text{C}) = 999.6987 \text{ kg/m}^3$ or $\rho(20^\circ\text{C}) = 998.2019 \text{ kg/m}^3$.

The calculated coefficients are given in Table 1 together with a polynomial of order five* from [26]. The resulting coefficients of thermal expansion vs temperature are shown in Fig. 5 whereas Fig. 6 shows the deviation $\beta' = d\beta/dT$ vs temperature. From these figures it is obvious that the polynomial (3.10) is not recommended. The differences in the results using the other polynomials are discussed later on.

Before proceeding further, it is appropriate to bring (1)–(4) into a dimensionless form by using H as reference length and ϑ as reference temperature where $\vartheta = T_1 - T_2$ for isothermal walls and $\vartheta = q_w H/\lambda$ if isoflux wall conditions are applied. With $\tau = at/H^2$ as dimensionless time (Fourier number) one obtains

$$\nabla \mathbf{u} = 0 \quad (8)$$

$$\frac{1}{Pr} \frac{D\mathbf{u}}{D\tau} = \mathbf{e} \cdot Ga \left(\frac{\rho}{\rho_0} - 1 \right) - \nabla P + \nabla^2 \mathbf{u} \quad (9)$$

$$\frac{D\theta}{D\tau} = \nabla^2 \theta \quad (10)$$

$$P = \rho(\theta)$$

where $\mathbf{e} = (0, 0, -1)$.

For steady state heat conduction the above system reduces to

$$\frac{\partial \bar{P}}{\partial z} = -Ga \left(\frac{\bar{\rho}}{\rho_0} - 1 \right) \quad (11)$$

$$\frac{\partial^2 \bar{\theta}}{\partial z^2} = 0.$$

With the boundary conditions

$$\bar{\theta}|_{z=0} = 0, \quad \bar{\theta}|_{z=1} = 1: \text{ constant wall temperature} \quad (12)$$

$$\left. \frac{d\bar{\theta}}{dz} \right|_{z=0,1} = -\frac{\dot{q}_w H}{\lambda(T_2 - T_1)}: \text{ constant wall heat flux}$$

one obtains the solution

$$\bar{\theta} = 1 - \frac{z}{H}. \quad (13)$$

By considering small perturbations of the conduction solution the solutions of (8), (9) and (10) can be expanded into the small parameter ε ; i.e.

$$\theta(\mathbf{x}, \tau) = \bar{\theta}(z) + \varepsilon \hat{\theta}(\mathbf{x}, \tau) + \dots$$

With similar expansions for \mathbf{u} and P and by equating terms of equal power in ε one obtains at $O(\varepsilon)$ the usual linearized perturbation equations

$$\nabla \cdot \hat{\mathbf{u}} = 0 \quad (14)$$

$$\frac{1}{Pr} \frac{\partial \hat{\mathbf{u}}}{\partial \tau} = \mathbf{e} \cdot Ra \cdot \theta \cdot \mathbf{f} - \nabla \hat{P} + \nabla^2 \hat{\mathbf{u}} \quad (15)$$

$$\frac{\partial \hat{\theta}}{\partial \tau} + \hat{\mathbf{w}} \frac{\partial \bar{\theta}}{\partial z} = \nabla^2 \hat{\theta} \quad (16)$$

with

$$\mathbf{f} = 1 + N_1 \bar{\theta} + N_2 \bar{\theta}^2 + N_3 \bar{\theta}^3 + \dots \quad (17)$$

It can be shown that the coefficients of nonlinearity are given by

$$N_i = \frac{1}{\beta} \frac{1}{i!} \beta^{(i)} (T_1 - T_2)^i. \quad (18)$$

The number of the nonlinearity-coefficients N_i is equal to $p - 1$.

Equations (14)–(15) can be reduced by eliminating the velocity components \hat{u} and \hat{v} and the pressure \hat{P} . After some manipulations which may be found elsewhere one ends up with two equations for the perturbation velocity component \hat{w} and the perturbation temperature $\hat{\theta}$,

$$\left(\frac{1}{Pr} \frac{\partial}{\partial \tau} - \nabla^2 \right) \nabla^2 \hat{w} = -Ra \cdot \mathbf{f} \cdot \nabla^2 \hat{\theta} \quad (19)$$

$$\left(\frac{\partial}{\partial \tau} - \nabla^2 \right) \hat{\theta} = \hat{w}. \quad (20)$$

* This polynomial is considered to be "exact" within the temperature range 0–40°C.

For $f = 1$, equation (19) reduces to that for the classical problem.

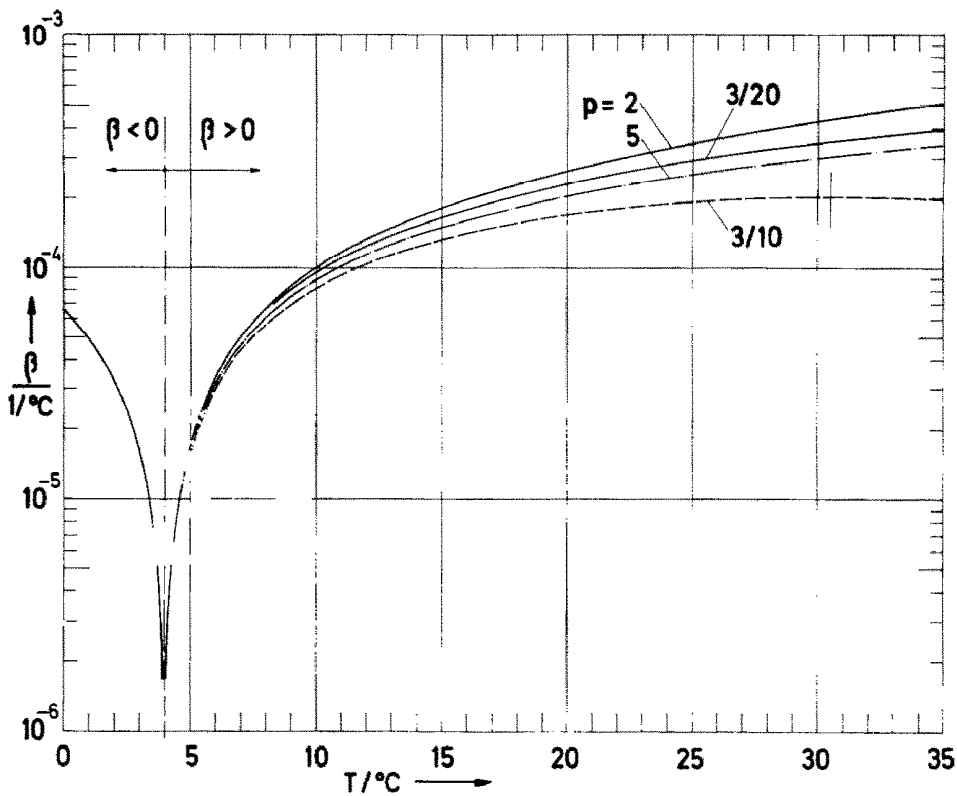


FIG. 5. Coefficient of thermal expansion vs temperature for different density-temperature polynomials (Table 1).

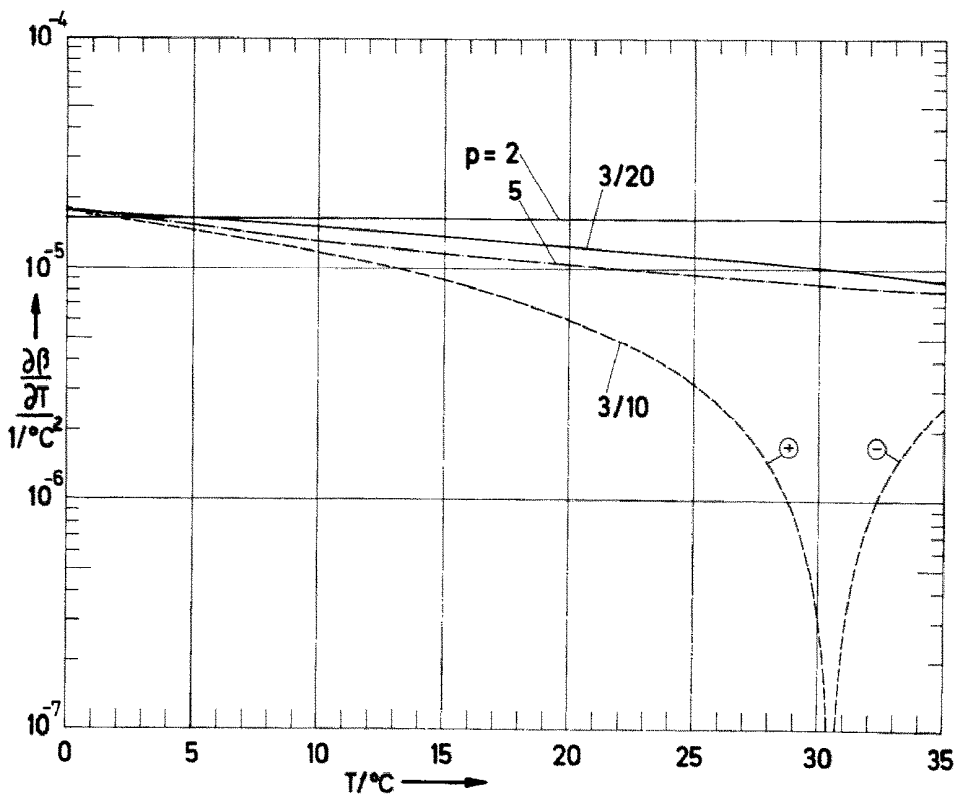


FIG. 6. First deviation of the coefficient of thermal expansion vs temperature for different density-temperature polynomials (Table 1).

3. METHOD OF SOLUTION

Only a very brief outline of the solution method will be given here. For details see Chandrasekhar [5], Denn [27] and Finlayson [28].

Since (19) and (20) are linear, the solution can be written as

$$\begin{aligned} \hat{w} &= F(z) \cdot H(x, y) \exp(\sigma\tau) \\ \hat{\theta} &= G(z) \cdot H(x, y) \exp(\sigma\tau). \end{aligned} \tag{21}$$

Putting (21) into (19) and (20) it can be seen that the resulting equations are separable if and only if

$$\nabla_2^2 H + k^2 H = 0. \tag{22}$$

Hence, the perturbations are periodic in x and y . Obeying (22), one obtains

$$\left[\frac{\sigma}{Pr} - (D^2 - k^2) \right] (D^2 - k^2) F = -k^2 Ra \cdot f \cdot G \tag{23}$$

$$[\sigma - (D^2 - k^2)] G = F. \tag{24}$$

Equations (23) and (24) describe an eigenvalue problem; i.e. solutions for $F(z)$ and $G(z)$ exist for certain combinations of $\{\sigma, k, Ra\}$ only. The eigenvalue σ , $\sigma = \sigma_r + i\sigma_i$ is a measure for the temporary decay, or increase, of the perturbation amplitudes. These amplitudes are amplified if $\sigma_r > 0$ and are damped if $\sigma_r < 0$; hence, $\sigma_r = 0$ denotes the case of neutral stability. It is said, that the principle of exchange of stability is valid if $\sigma_i = 0$ as $\sigma_r = 0$. This

The eigenfunctions $F(z)$ and $G(z)$ are approximated by

$$\begin{aligned} F(z) &= \sum_{l=1}^L C_l \phi_l(z) \\ G(z) &= \sum_{m=1}^M D_m \psi_m(z) \end{aligned} \tag{25}$$

where each of the test functions $\phi_l(z)$ and $\psi_m(z)$ satisfies the boundary conditions.

Substituting (25) in (23) and (24) results in a residual in each of the equations because (25) is not a solution of (23) and (24). The essence of Galerkin's method is now to establish equations for the coefficients C_l and D_m by requiring that the residuals be orthogonal to each of the approximating functions,

$$\int_{z=0}^1 \text{Res}_1 \{ C_l, D_m \} \phi_p(z) dz = 0; \tag{26}$$

$$p = 1, \dots, L$$

$$\int_{z=0}^1 \text{Res}_2 \{ C_l, D_m \} \psi_q(z) dz = 0; \tag{26}$$

$$q = 1, \dots, M.$$

Equations (26) are a set of $L+M$ linear, homogeneous algebraic equations for the C_l and D_m . One obtains, after substituting (23), (24) and (25) into (26), integrating by parts and rearranging the result

$$\begin{bmatrix} A_{00}^{11} & \dots & A_{L0}^{11} & | & A_{00}^{12} & \dots & A_{M0}^{12} \\ \vdots & & \vdots & | & \vdots & & \vdots \\ A_{0L}^{11} & \dots & A_{LL}^{11} & | & A_{0L}^{12} & \dots & A_{ML}^{12} \\ \hline A_{00}^{21} & \dots & A_{L0}^{21} & | & A_{00}^{22} & \dots & A_{M0}^{22} \\ \vdots & & \vdots & | & \vdots & & \vdots \\ A_{0M}^{21} & \dots & A_{LM}^{21} & | & A_{0M}^{22} & \dots & A_{MM}^{22} \end{bmatrix} \begin{bmatrix} C_0 \\ \vdots \\ C_L \\ \dots \\ D_0 \\ \vdots \\ D_M \end{bmatrix} = 0 \tag{27}$$

is sometimes also called the point of marginal stability. For $\sigma_i \neq 0$ as $\sigma_r = 0$ oscillatory instabilities occur which are sometimes called over-stabilities. To the author's knowledge no general proof that σ is real has yet been carried out for the present case. Merker *et al.* [29] have merely shown that there may exist solutions with $\sigma_i \neq 0$ as $\sigma_r = 0$. Nevertheless, in seeking a solution we shall assume that σ is real. The point of marginal stability is therefore achieved by setting $\sigma = 0$. It may be noted that the Prandtl number disappears for $\sigma = 0$ from (25), and the eigenvalue problem reduces to $\{k, Ra\} = 0$.

For solid walls the hydrodynamic boundary conditions are given with $F = F' = 0$. The thermal boundary condition gives $G = 0$ for isothermal walls and $G' = 0$ for constant wall heat flux.

Equations (25) and (26) are solved for $\sigma = 0$ using Galerkin's method, see Finlayson [28] for example.

with the coefficients

$$\begin{aligned} A_{lp}^{11} &= I_{lp}^2 + 2k^2 I_{lp}^1 + k^4 I_{lp}^0 \\ A_{mp}^{12} &= k^2 Ra \int_{z=0}^1 f \cdot \psi_m \cdot \phi_p dz \\ A_{lq}^{21} &= - \int_{z=0}^1 \phi_l \psi_q dz \\ A_{mq}^{22} &= K_{mq}^1 + k^2 K_{mq}^0, \end{aligned} \tag{28}$$

where the integrals are given by

$$\begin{aligned} I_{lp}^i &= \int_{z=0}^1 \phi_l^{(i)} \phi_p^{(i)} dz; \quad i = 0, 1, 2 \\ K_{mq}^i &= \int_{z=0}^1 \psi_m^{(i)} \psi_q^{(i)} dz; \quad i = 0, 1. \end{aligned} \tag{29}$$

A nonzero solution exists if and only if the determinant of coefficients vanishes. This happens for certain combinations of the values Ra and k only.

Hence, from

$$\text{DET}[A(k, Ra; N_i)] = 0 \quad (30)$$

follows for the minimum (critical) Rayleigh number Ra_1 (or Ra_2)

$$Ra_1 = \text{MIN}[Ra(k; N_i)]. \quad (31)$$

Using a procedure described by Finlayson [28], one obtains the testfunctions

$$\phi_l = (1-z)^2 \cdot z^{2+l} \quad (32)$$

$$\psi_m = (1-z)z^{1+m} \quad : \quad T_w = \text{const.} \quad (33)$$

$$\psi_m = 1 + (1-z)^2 \cdot z^{2+m} \quad : \quad \dot{q}_w = \text{const.}$$

It can easily be shown that each of these testfunctions satisfies the boundary conditions. With these testfunctions the coefficients (28) and (29) are actually calculated with $L = M = n$ terms.

4. RESULTS

It can be seen from the general diagram of stability, Fig. 4, that the Rayleigh number Ra_1 is always defined as positive if the layer is unstably stratified whereas the Rayleigh number Ra_2 changes sign. Hence, it appears reasonable to describe the stability of a layer by using Ra_1 instead of Ra_2 .

The calculated critical Rayleigh numbers using $p = 5$ and $n = 7$ are shown in Fig. 7 for the boundary condition $T_w = \text{const.}$ and in Fig. 8 for $\dot{q}_w = \text{const.}$ The convergence of the Galerkin method has been proved by comparing the calculated Rayleigh numbers with those obtained by using $n = 9, 11$ and 14 terms instead of 7 . From this, it can be concluded that the approach with $n = 7$ is close to 1% in the temperature region -6 to $+40^\circ\text{C}$ except the asymptotic region near 4°C where $Ra_1 > 10^5$.

The region below the isotherm $T_2 = 4^\circ\text{C}$ refers to a density profile with no maximum value, i.e. the complete layer is unstably stratified. For this case, it can be said, the bending of the density profile is weak, and accordingly, the effect on the critical Rayleigh number is small. The calculated Rayleigh

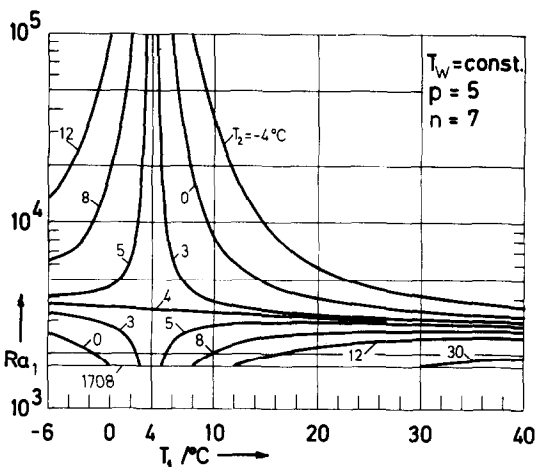


FIG. 7. Critical Rayleigh number vs temperature T_1 (bottom) for $T_w = \text{const.}$

numbers are between 1708 and about 3600 for $T_w = \text{const.}$ and between 720 and about 1600 for $\dot{q}_w = \text{const.}$

The region above the isotherm $T_2 = 4^\circ\text{C}$ refers to a density profile with maximum value, i.e. only a part of the layer is unstably stratified. The bending of the profile is called strong and the effect on the critical Rayleigh number is considerable. The Rayleigh numbers are remarkably bigger than those obtained for the classical problem. One may become more familiar with the stability diagrams in Fig. 7 and 8 by considering the following two cases.

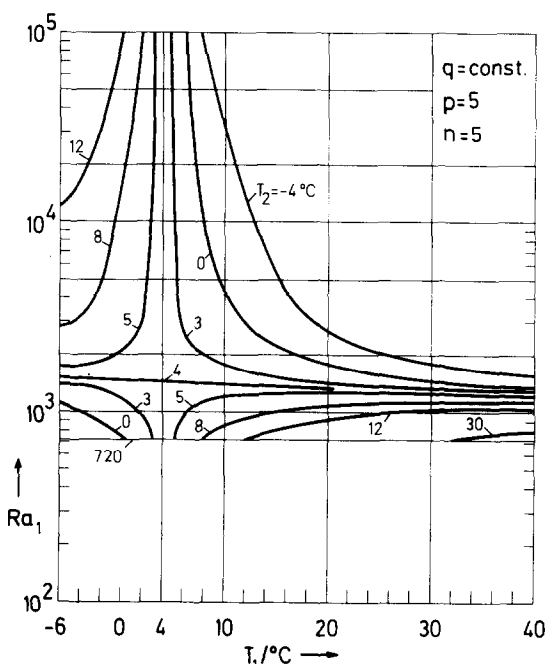


FIG. 8. Critical Rayleigh numbers vs temperature T_1 (bottom) for $\dot{q}_w = \text{const.}$

1. Temperature of the upper wall is $T_2 < 4^\circ\text{C}$, for example $T_2 = 0^\circ\text{C}$: Cooling this water layer with $T_1 < 0^\circ\text{C}$ from below results in an unstable stratification, where the bending of the profile is weak. The water layer is stable if heated from below with temperatures $0 \leq T_1 \leq 4^\circ\text{C}$ and it becomes partially unstable if T_1 exceeds 4°C . The density profile includes then the maximum density and the bending of the profile is strong.

2. Temperature of the upper wall is $T_2 > 4^\circ\text{C}$; for example $T_2 = 8^\circ\text{C}$: If this layer is cooled from below with $T_1 < 4^\circ\text{C}$ the upper part between the upper wall and the 4°C -isotherm remains stable whereas the lower part becomes unstable. The strong bending of the profile affects the Rayleigh number considerably.

The layer is stable if cooled with temperature T_1 between 4 and 8°C .

The layer is unstably stratified if heated from below with $T_1 > 8^\circ\text{C}$. As the bending of the profile is weak the Rayleigh number remains in the region between 1700 and 3600.

5. SOME COMMENTS ON THE APPROACH WITH THE FIRST GALERKIN TERM ONLY

It has been shown so far that the critical Rayleigh number depends on the wall temperatures, T_1 and T_2 . It can be seen from Fig. 9 that this is also true for the critical wave number. The diagram shows that the critical wave number is equal to 3.11 for density profiles excluding the point of maximum density and it increases as the bending increases for profiles including the point of maximum density. As the wave number is inversely proportional to the size of the resulting convection cells, the cell size increases as the height of the unstable layer increases. This result is what one would expect.

Coming to the point now, it follows from (27) for $n = 1$

$$Ra = \frac{(I_{00}^2 + 2k^2 I_{00}^1 + k^4 I_{00}^0) \cdot (K_{00}^1 + k^2 K_{00}^0)}{k^2 \int_{z=0}^1 f(\psi_0)^2 dz \cdot \int_{z=0}^1 \phi_0 \psi_0 dz} \quad (34)$$

The minimum (critical) Rayleigh number is obtained as

$$(I_{00}^2 + 2k^2 I_{00}^1 + k^4 I_{00}^0) \times (K_{00}^1 + k^2 K_{00}^0) / k^2 \rightarrow \text{MIN.} \quad (35)$$

For $n = 1$, the integrals I_{00}^1 and K_{00}^1 are mere numbers. Hence, from (35) follows that the minimum (critical) wave number is a constant which does not depend on the curvature of the density profile.

For that reason the approach with the first term only is limited to regions where $k_c \approx \text{const.}$, see Fig. 9.

6. COMPARING POLYNOMIALS OF ORDER 2, 3 AND 5 AS APPROXIMATIONS FOR THE DENSITY-TEMPERATURE FUNCTION

As mentioned above, we consider the Rayleigh numbers calculated with the 5th order polynomial as exact. Hence, the following errors can be defined

$$\begin{aligned} Ra_{ex} &\equiv Ra|_{n=5}^p \\ f_{7,2} &= (Ra|_{n=7}^p - Ra_{ex}) / Ra_{ex} \\ f_{7,3} &= (Ra|_{n=3}^p - Ra_{ex}) / Ra_{ex} \\ f_{1,2} &= (Ra|_{n=2}^p - Ra_{ex}) / Ra_{ex} \\ f_{1,5} &= (Ra|_{n=1}^p - Ra_{ex}) / Ra_{ex} \end{aligned}$$

Figure 10 shows these errors $f_{n,p}$ vs T_1 for $T_2 = 0^\circ\text{C}$. It can be seen that the calculated Rayleigh numbers using the parabolic polynomial are on an average about 10% too large. This error reduces to about 3% if a cubic term is added to the temperature density relation.

The approach with the first term only and a parabolic relation results in an average error $f_{1,2}$ of about 20%. Furthermore, it is interesting to note that the errors resulting from the neglected higher order Galerkin terms and that from the neglected higher order terms in the density-temperature polynomial compensate each other so that one obtains $f_{1,2} < f_{1,5}$ as $T_1 > 25^\circ\text{C}$. In addition, it can be seen that the approach with the first Galerkin term is

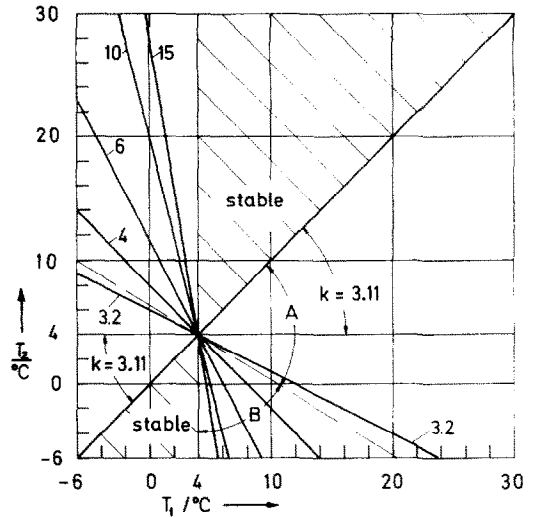


FIG. 9. Curves of constant critical wave number k in a $T_1 - T_2$ temperature chart. (A) Region where the approximation with the first term only ($n = 1$) gives reasonable results. (B) Region where higher order terms are needed (approx. 7) to achieve reasonable results.

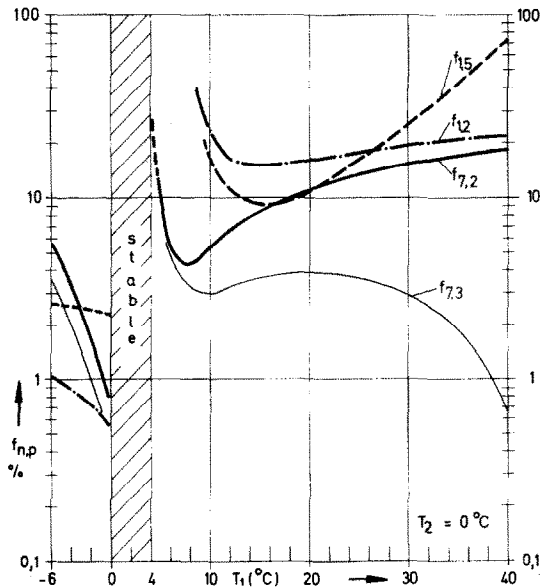


FIG. 10. Errors $f_{n,p}$ vs temperature T_1 for $T_2 = 0^\circ\text{C}$ and isothermal walls.

completely false near the density maximum. The errors $f_{1,2}$ and $f_{1,5}$ tend to infinity as T_1 approaches 8°C and 0°C , respectively. Figure 11 shows the errors $f_{n,p}$ vs T_1 for $T_2 = 8^\circ\text{C}$. In opposition to the case shown in Fig. 10 the bending of the density profile is weak for $T_1 > 8^\circ\text{C}$ and accordingly, the resulting errors are smaller. Principally, what has been said to Fig. 10 is valid for this case too.

7. ANALOGY BETWEEN FLUIDS HAVING A DENSITY ANOMALY AND THOSE HAVING INTERNAL HEAT SOURCES

The problem of the onset of convection due to internal heat sources has been treated by Sparrow *et al.* [30], Suo-Anttila *et al.* [31], Pnueli [32] and Cheung [33].

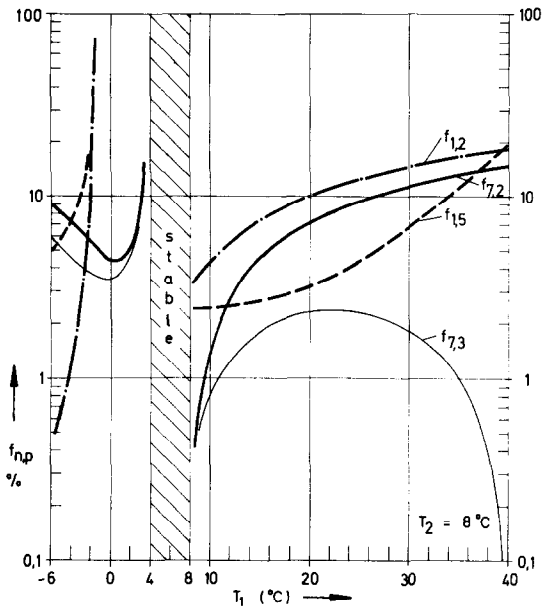


FIG. 11. Errors $f_{n,p}$ vs temperature T_1 for $T_2 = 8^\circ\text{C}$ and isothermal walls.

It will be shown in this chapter that the predicted stability diagram for fluids with density maximum is identically valid for those having internal heat sources.

(a) The temperature profile in a horizontal fluid layer having homogeneously distributed heat sources Q is given by Fourier's law

$$\frac{\partial^2 T}{\partial z^2} = \frac{Q}{\lambda}$$

From this follows for the temperature profile according to the boundary conditions $T(z=0) = T_1$ and $T(z=H) = T_2$,

$$T = \frac{Qz^2}{2\lambda} - \frac{QH}{2\lambda}z + (T_2 - T_1)\frac{z}{H} + T_1$$

For a normal fluid the density is a linear function of temperature, hence

$$\frac{\rho}{\rho_0} - 1 = -\beta_0(T - T_0)$$

Combining the last two equations gives

$$\frac{\rho}{\rho_0} - 1 = -\beta_0 \left[T_1 - T_0 + (T_2 - T_1)\frac{z}{H} - \frac{QH^2}{2\lambda} \frac{z}{H} - \frac{QH^2}{2\lambda} \left(\frac{z}{H}\right)^2 \right] \quad (36)$$

(b) If there are no heat sources present, the temperature profile reduces to the linear one $T = (T_2 - T_1)(z/H) + T_1$.

Introducing the nonlinear density-temperature relation

$$\frac{\rho}{\rho_0} - 1 = B_1 T + B_2 T^2 + \dots$$

leads to

$$\begin{aligned} \frac{\rho}{\rho_0} - 1 &= B_1 T_1 + B_2 T_1^2 \\ &+ [B_1(T_2 - T_1) + 2B_2 T_1(T_2 - T_1)] \cdot \frac{z}{H} \\ &+ B_2(T_1 - T_2)^2 \left(\frac{z}{H}\right)^2 \end{aligned} \quad (37)$$

Equating terms of like power in z in (36) and (37), one obtains for the unknown coefficients B_1 , B_2 and T_0

$$\begin{aligned} B_1 &= \beta_0 \left[\frac{QH^2}{2\lambda} \frac{T_1 + T_2}{(T_1 - T_2)^2} - 1 \right] \\ B_2 &= -\frac{QH^2}{2\lambda} \frac{\beta_0}{(T_1 - T_2)^2} \\ T_0 &= \frac{QH^2}{2\lambda} \frac{T_1 T_2}{(T_1 - T_2)^2} \end{aligned} \quad (38)$$

It follows for the "fictive" nonlinearity, equation (18)

$$N_1 = \frac{2B_2 \vartheta}{B_1 + 2B_2 T_0}$$

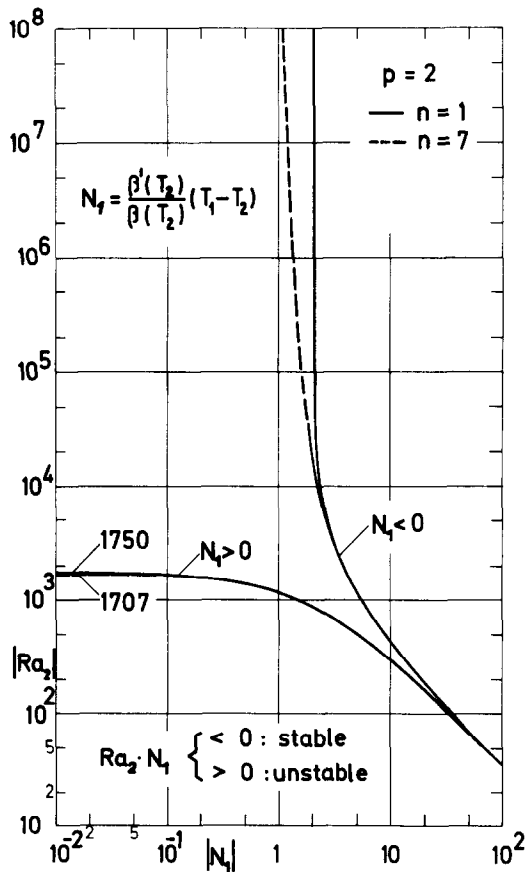


FIG. 12. Rayleigh number Ra_2 vs nonlinearity N_1 for a parabolic density-temperature relation and $T_w = \text{const}$. $N_1 > 0$: complete layer is unstably stratified. $N_1 < 0$: only lower part is unstably stratified.

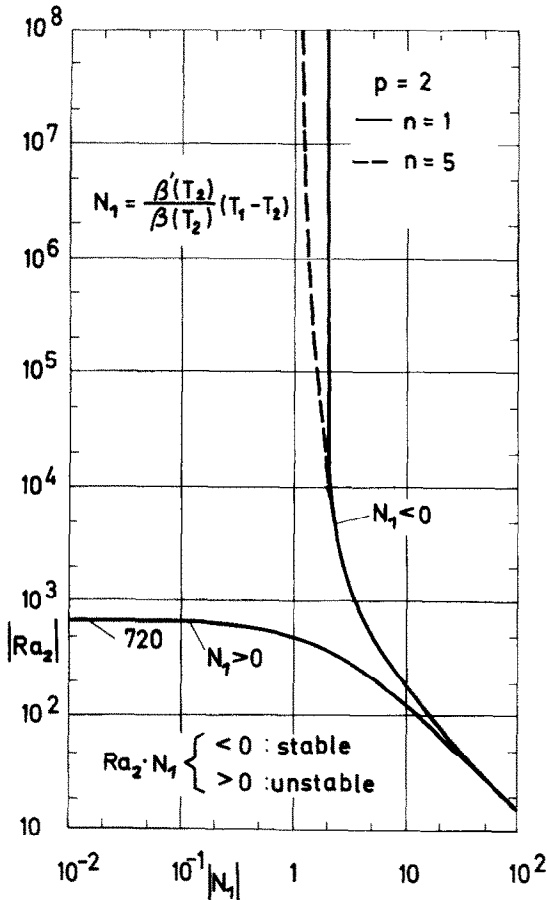


FIG. 13. Rayleigh number Ra_2 vs nonlinearity N_1 for parabolic density-temperature relation and $\dot{q}_w = \text{const}$. $N_1 > 0$: complete layer is unstably stratified. $N_1 < 0$: only lower part is unstably stratified.

after substituting the coefficients (38)

$$N_1 = \frac{2\kappa}{1 - \kappa \frac{T_1 + T_2}{T_1 - T_2} + 2\kappa^2 \frac{T_1 T_2}{(T_1 - T_2)^2}} \quad (39)$$

where $\kappa = QH^2/[2\lambda(T_1 - T_2)]$.

Therefore, the dimensionless diagrams, Figs. 12 and 13 describe the onset of convection in a horizontal fluid layer having a nonlinear density temperature relation, as well as in a fluid layer with homogeneous distributed heat sources. One should keep in mind that the comments in Chapter 6 concerning the approach with the first Galerkin's term refer also to the case with internal heat sources.

In principle, the case with a nonhomogeneous heat source, i.e. $Q = Q(z)$ can be treated correspondingly. One obtains expressions for the "higher" nonlinearities N_i with $i \geq 2$, but the stability diagrams cannot be presented in the same simple way.

REFERENCES

1. J. Straub, G. Merker, K. Küblbeck, A. Staudt and U. Grigull, Untersuchung der Konvektion in Jahresspeichern. *VDI-Berichte* **288**, 39-46 (1977).

2. H. Bénard, Les Tourbillons cellulaires dans une nappe liquide. *Rev. Gen. Sci. Pures Appl.* **11**, 1261-1271 (1900).
3. Lord Rayleigh, On convective currents in a horizontal layer of fluid when the higher temperature is on the under side. *Phil. Mag.* **32**, 529-46 (1916).
4. H. Jeffreys, The stability of a layer of fluid heated below. *Phil. Mag.* **2**, 833-844 (1926).
5. S. Chandrasekhar, *Hydrodynamic and Hydromagnetic Stability*. Clarendon Press, Oxford (1961).
6. E. L. Koschmieder, Bernard convection. *Adv. Chem. Phys.* **26**, 177-212 (1974).
7. D. D. Joseph, *Stability of Fluid Motion*, Vol. 2. Springer, Berlin (1976).
8. G. Veronis, Penetrative convection. *Astrophys. J.* **137**, 641-663 (1963).
9. Z. S. Sun, C. Tien and Y. -C. Yen, Thermal instability of a horizontal layer of liquid with maximum density. *A.I.Ch.E. J.* **15**, 910-915 (1969).
10. N. Seki, S. Fukusako and M. Sugawara, A criterion of onset of free convection in a horizontal melted water layer with free surface. *J. Heat Transfer* **99**, 92-98 (1977).
11. J. C. Legros, D. Longree and G. Thomaes, Bénard problem in water near 4°C. *Physica* **12**, 410-414 (1974).
12. R. S. Wu and K. C. Cheng, Maximum density effects on thermal instability by combined buoyancy and surface tension. *Int. J. Heat Mass Transfer* **19**, 559-565 (1976).
13. D. V. Boger and J. W. Westwater, Effect of buoyancy on the melting and freezing process. *J. Heat Transfer* **89**, 81-89 (1967).
14. Y. -C. Yen, Onset of convection in a layer of water formed by melting ice from below. *Physics Fluids* **11**, 1263-1270 (1968).
15. Y. -C. Yen and F. Galea, Onset of convection in a water layer formed continuously by melting ice. *Physics Fluids* **12**, 509-516 (1969).
16. R. S. Tankin and R. Farhadieh, Effects of thermal convection currents on formation of ice. *Int. J. Heat Mass Transfer* **14**, 953-961 (1971).
17. R. Faradieh and R. S. Tankin, A study of the freezing of sea water. *J. Fluid Mech.* **71**, 293-304 (1975).
18. N. Seki, S. Fukusako and M. Sugawara, Free convective heat transfer and criterion of onset of free convection in a horizontal melt layer of ice heated by upper rigid surface. *Wärme- und Stoffübertragung* **10**, 269-279 (1977).
19. G. P. Merker, P. Waas and U. Grigull, Einsetzen der Konvektion in einer von unten gekühlten Wasserschicht bei Temperaturen unter 4°C. *Wärme- und Stoffübertr.* **9**, 99-110 (1976).
20. R. B. Bird, W. E. Stewart and E. N. Lightfoot. *Transport Phenomena*. John Wiley and Sons, New York (1960).
21. F. M. White, *Viscous Fluid Flow*. McGraw-Hill, New York (1974).
22. E. Heß, Freie Konvektion von Luft im horizontalen Ringspalt bei temperatur- und druckabhängiger Dichte. Diss., Ruhr Univers. Bochum (1971).
23. D. D. Gray and A. Giorgini, The validity of the Boussinesq approximation for liquids and gases. *Int. J. Heat Mass Transfer* **19**, 545-551 (1976).
24. J. R. Booker, Thermal convection with strongly temperature-dependent viscosity. *J. Fluid Mech.* **76**, 741-754 (1976).
25. G. S. Kell, and E. Whalley, Reanalysis of the density of liquid water in the range 0-150°C and 0-1 kbar. *J. Chem. Phys.* **62**, 3496-3503 (1975).
26. H. Wagenbreth and H. Blanke, Die Dichte des Wassers im Internationalen Einheitensystem und in der Internationalen Praktischen Temperaturskala von 1968. *PTB-Mitteilungen* **6**, 412-415 (1971).
27. M. M., Denn, *Stability of Reaction and Transport Processes*. Prentice-Hall, Englewood Cliffs, New Jersey (1975).

28. B. A. Finlayson, *The Method of Weighted Residuals and Variational Principles*. Academic Press, New York (1972).
29. G. P. Merker, Einfluß der Dichteanomalie von Wasser auf das Einsetzen der Konvektion einer von unten beheizten bzw. gekühlten halbunendlichen Schicht, *Wärme- und Stoffübertragung* **10**, 255–267 (1977).
30. E. M. Sparrow, R. J. Goldstein and V. K. Jonsson, Thermal instability in a horizontal fluid layer: effect of boundary conditions and non-linear temperature profile, *J. Fluid Mech.* **18**, 513–528 (1963).
31. A. J. Suo-Anttila and I. Catton, The effect of a stabilizing temperature gradient on heat transfer from a molten fuel layer with volumetric heating, in *ASME Winter Annual Meeting*, New York, 17–22 November (1974).
32. D. Pnueli, Thermal instability under variable initial temperature gradient, *Letters Heat Mass Transfer* **2**, 495–504 (1975).
33. F. B. Cheung, Natural convection in a volumetrically heated fluid layer at high Rayleigh numbers, *Int. J. Heat Mass Transfer* **20**, 499–506 (1977).

CONVECTION DANS UNE COUCHE D'EAU HORIZONTALE AVEC EFFET DE DENSITE MAXIMALE

Résumé—On étudie la convection dans une couche d'eau horizontale en considérant l'anomalie de densité (près de 4°C) et en utilisant l'analyse de stabilité linéaire. Les équations de perturbation sont résolues à l'aide de la méthode de Galerkin. Avec le choix de fonctions convenables, on montre que 7 termes sont suffisants pour une approche voisine de 1%. Les résultats sont représentés par des diagrammes de stabilité, $Ra = Ra(T_1, T_2)$ où T_1 et T_2 sont les températures respectives des parois inférieures et supérieures. La relation non linéaire entre densité et température est approchée par trois polynômes différents ayant 2, 3 et 5 termes. Supposant exact le polynôme du cinquième ordre, les nombres de Rayleigh critiques calculés avec la simple relation parabolique sont trop élevés d'environ 10%. Cet écart est réduit à approximativement +3% en ajoutant un terme cubique à cette relation densité-température.

Zusammenfassung—Es wird der Einfluß der nichtlinearen Dichte-Temperatur-Beziehung von Wasser in der Nähe der Dichteanomalie bei etwa 4°C auf das Einsetzen der Konvektion in einer horizontalen Schicht untersucht. Die linearen Stördifferentialgleichungen werden mit dem Galerkin Verfahren gelöst. Bei geeigneter Wahl der Testfunktionen genügen 7 Terme der Galerkin-Entwicklung für eine Genauigkeit von etwa 1%. Die berechneten kritischen Rayleigh-Zahlen sind in Stabilitäts-Diagrammen als Funktion der Temperaturen T_1 (Unterseite) und T_2 (Oberseite) dargestellt. Die nichtlineare Dichte-Temperatur-Beziehung wird durch Polynome mit 2 (Parabel), 3 und 5 Termen angenähert. Es wird gezeigt, daß die mit der einfachen Parabel berechneten Rayleigh-Zahlen gegenüber dem als "exakt" angenommenen Polynom mit 5 Termen im Mittel um etwa 10% groß sind. Durch Hinzunahme eines kubischen Terms reduziert sich dieser Fehler auf etwa +3%.

ВОЗНИКНОВЕНИЕ КОНВЕКЦИИ В ГОРИЗОНТАЛЬНОМ СЛОЕ ВОДЫ ПРИ МАКСИМАЛЬНОМ ЗНАЧЕНИИ ПЛОТНОСТИ

Аннотация—С помощью линейного анализа устойчивости исследуется возникновение конвекции в горизонтальном слое воды с учётом аномалии её плотности при 4°C. Полученные уравнения возмущений решаются методом Галёркина. Соответствующим выбором необходимых пробных функций показано, что для получения соответствия в 1% достаточно семи членов. Результаты представлены в виде диаграмм устойчивости $Ra = Ra(T_1, T_2)$, где T_1 и T_2 — соответственно температура нижней и верхней стенок. Нелинейное соотношение между плотностью и температурой аппроксимируется тремя различными полиномами с 2, 3 и 5 членами. При условии, что полином 5-го порядка является точным, получаем, что вычисление критического значения числа Релея с помощью простого параболического соотношения завышает его на 10%. Это завышение снижается примерно до +3% добавлением кубического слагаемого в температурную зависимость плотности.